PCCP

RSC Publishing

PAPER

View Article Online
View Journal | View Issue

Published on 27 March 2013. Downloaded by Ruhr Universitat Bochum on 1/16/2019 10:21:45 AM.

Cite this: *Phys. Chem. Chem. Phys.*, 2013, **15**, 7567

Computational screening of one- and two-photon spectrally tuned channelrhodopsin mutants†

Kristian Sneskov,[a] Jógvan Magnus Haugaard Olsen,*[b] Tobias Schwabe,[c] Christof Hättig,[d] Ove Christiansen[a] and Jacob Kongsted[b]

Received 4th December 2012,
Accepted 26th March 2013

DOI: 10.1039/c3cp44350g

www.rsc.org/pccp

Optogenetics is by now a well-established field within neuroscience where neuro-response is controlled at the molecular level using the photochemical properties of channelrhodopsin (ChR). In this study the recently published X-ray structure of retinal inside the ChR binding pocket serves as the basis for conducting high-level polarizable embedding quantum mechanical/molecular mechanical (QM/MM) mutation studies with the aim of providing insight into the tuning mechanisms of this remarkable protein. The levels of theory applied are the recently developed PERI-CC2 and PE-DFT approaches. Their computational efficiency makes it possible to rapidly carry out a large number of spectral calculations. This is exploited to construct *in silico* mutated ChR variants which are characterized in terms of the location of the relevant excitation energy and the magnitude of the two-photon absorption cross section. In turn, this allows us to pinpoint the amino acids that have the largest electrostatic effect on the studied excited state properties. We show that a single/double site mutation strategy in ChR does not perturb the electronic properties of retinal to a degree that satisfies the experimental demand for a significant red-shift. With respect to non-linear absorption we conjecture that the recently synthesized ChETA variant possesses an even larger two-photon cross section than the C1C2 variant and it is thus an ideal candidate for further studies on the two-photon activation of ChR.

1 Introduction

In 2005, K. Deisseroth and co-workers[1,2] sparked a revolution within neuroscience, called optogenetics[3] (chosen as the method of the year in 2010 by *Nat. Methods*[4]), by offering scientists an unprecedented level of control of neuro-response at the molecular level. The responsible molecular tool is the non-selective cation-channel channelrhodopsin (ChR). It is a member of a larger family of 7-*trans*-membrane proteins – generally referred to as opsins – all sharing one important property: the ability to be activated (opened) upon stimulation by light. In ChR the photocycle is initiated by a light-absorbing chromophore – *all-trans* retinal – bonded to the Lys296 residue *via* a protonated Schiff-base. We shall throughout denote this retinylidene Schiff base chromophore simply as the retinal chromophore. In practice, a few different naturally occurring ChR variants have been found, of which ChR1 and ChR2 from *Chlamydomonas reinhardtii* are the most important for optogenetic experiments.[5] Especially ChR2 has found widespread applications because of its relative ease of expression in different host organisms while still giving rise to detectable photocurrents. However, for many biological applications ChR2 remains a relatively blunt tool and calls for red-shifted ChRs.[6] For instance, at the activation wavelength of approximately 2.70 eV the absorption and scattering coefficients of biological tissue are very high, naturally complicating its straightforward use in brain tissue. Another appealing consequence of engineering absorption shifted ChRs is the potential to ''enable control of two separate populations within the same physical volume''.[7]

With the aim of improving the photochemical properties of ChR, many different strategies have been pursued including site-directed mutagenesis as well as helix swapping to create ChR chimeras.[8–13] In turn, this has led to the design and synthesis of a plethora of ChR variants each differing slightly

[a] *The Lundbeck Foundation Center for Theoretical Chemistry and Center for Oxygen Microscopy and Imaging, Department of Chemistry, University of Aarhus, Langelandsgade 140, 8000 Aarhus C, Denmark*
[b] *Department of Physics, Chemistry and Pharmacy, University of Southern Denmark, Campusvej 55, 5230 Odense M, Denmark. E-mail: jmo@sdu.dk; Fax: +45 66158780; Tel: +45 65502570*
[c] *Center for Bioinformatics and Institute of Physical Chemistry, University of Hamburg, Bundesstraße 43, 20146 Hamburg, Germany*
[d] *Lehrstuhl für Theoretische Chemie, Ruhr-Universität Bochum, 44801 Bochum, Germany*

† Electronic supplementary information (ESI) available. See DOI: 10.1039/c3cp44350g

Published on 27 March 2013. Downloaded by Ruhr Universitat Bochum on 1/16/2019 10:21:45 AM.

in their physical properties. With the aim of understanding the factors that determine the properties of ChR, a 2.3 Å resolved crystal structure of a ChR1 and ChR2 chimera, called C1C2, was recently reported[14] yielding a very detailed picture of the binding pocket of ChR2. As recognized by several authors[3,5,6] this is an important first step towards a deeper understanding of the factors governing the properties of ChR allowing for more principled and accurate tuning (and understanding) of ChR properties. Here, we take the next logical step by dissecting the factors influencing the spectral properties of ChR. We use a systematic approach to the study of spectral tuning: by detailing the spectral effect of the amino acids constituting the binding pocket we may use computational methods to effectively screen a large set of mutants in order to elucidate the possibilities of spectrally tuning ChR using point mutations. We believe this is a vital tool in the continued quest for engineering rationally designed photosensitive proteins. Related studies already followed similar approaches and showed promising results.[15,16] Here, the general approach is improved with a more detailed description of the protein surrounding by a polarizable embedding potential and by also considering two-photon absorption properties. A theoretical investigation on its own does of course not guarantee that the mutant is available for experiments. For instance, the given amino acid substitution might cause the protein to fold differently. Another practical concern is whether the ChR variant is still expressed in neurons. Still, the results illustrate the possibilities offered by state-of-the-art quantum chemistry methods for enhancing ChR as an optogenetic tool.

At the frontier of optogenetic experiments is the use of two-photon techniques to activate the channel.[17,18] Especially, two-photon cross sections of remarkable size have been reported.[17] The appealing properties – especially for application to biological tissues – include the use of IR wavelengths thus paving a way for overcoming the scattering challenge and allowing for much larger penetration depths. Additionally, the non-linear nature of two-photon absorption results in control of the size of the focal (excitation) volume and even prospects of single neuron studies. It is thus clear that the development of two-photon activation tools is another important focus area needed to expand the optogenetic toolbox.[7] In order to meet this challenge, we here also investigate the potential for tuning the size of the two-photon cross section by demonstrating how we may screen a set of mutants for two-photon activity.

Both isolated retinal and retinal in different protein environments have been studied using numerous methods in dozens of papers. A full listing is not relevant here and we only refer to a few studies as an entry to this literature.[19–30] It should be emphasized that the reliability of the approximate coupled cluster singles and doubles approach (CC2) for excitation energies of the retinal chromophore as well as related studies in which the influence of the protein is taken into account has been demonstrated before.[31–36] Here, we make use of the newly developed polarizable embedding CC2 method including the resolution of the identity approximation (PERI-CC2).[37]

The paper is organized as follows: in the second section we start out with some basic considerations of modelling electronic excitations in biological chromophores including some important aspects of the polarizable embedding density functional theory[38] (PE-DFT) and PERI-CC2 methods. Thereafter, we describe the technical details of the computations, including the protocol used for performing the mutation studies. Then, we present the results and discuss their significance for tuning ChR for optogenetic experiments.

2 Polarizable embedding: the PERI-CC2 and PE-DFT approaches

The combined quantum mechanics/molecular mechanics (QM/MM) approach[39] for treating large molecular systems relies on the fundamental chemical principle that some regions of the molecular system are chemically more important than others. Explicitly, the system is partitioned into two interacting regions treated either quantum mechanically or using more computationally efficient classical mechanics methods. In ChR this partitioning is quite naturally retinal (QM) and the amino acids (MM) constituting the full protein. The interaction between the subsystems is then accounted for in an effective manner by introducing proper coupling terms in the quantum chemistry equations describing the QM region. In the polarizable embedding (PE) approach[38,40,41] to QM/MM the ground state total energy is given as

$$L_{\mathrm{PE}} = \left\langle \hat{H}^{\mathrm{QM}} \right\rangle + \left\langle \hat{G}^{\mathrm{es}} \right\rangle - \frac{1}{2}\sum_{uv} F_u(\boldsymbol{D}) R_{uv} F_v(\boldsymbol{D}) + E^{\mathrm{MM}}. \quad (1)$$

Here $\langle \hat{H}^{\mathrm{QM}} \rangle$ is the standard vacuum-like Hamiltonian contribution from the QM subsystem. The coupling operator $\hat{G}^{\mathrm{es}}$ includes the interaction of the classical multipoles in the MM system with the QM electronic density. The third term is the self-consistently induced dipole interaction with the QM subsystem describing many-body induction (polarization) effects. This term depends on the electronic density quadratically. Finally, the fourth term includes all those terms that do not affect the electronic wave function calculations, and thus they do not need to be discussed further here. We refer to the previous works for the detailed definition.[37,38,40,41] Importantly, the PE approach ensures that both the electrostatic interaction (second term) and the mutual polarization of the QM and MM parts (third term) are incorporated not only in the ground state wavefunction optimization but also in the calculation of one- and two-photon excitation properties. In the study of electronic transitions it is crucial to consider the effects of a changing electronic structure upon excitation for the interaction between the QM and MM subsystems.[42] In the mathematical language of response theory the derivatives of a suitably defined Lagrangian define the effective eigenvalue equations that ultimately determine the excitation energies and transition properties. These effective eigenvalue equations thereby implicitly include effects accounting for the changing density upon electron excitation. Such terms are

 This journal is © the Owner Societies 2013

Published on 27 March 2013. Downloaded by Ruhr Universitat Bochum on 1/16/2019 10:21:45 AM.

included in PE theory through the derivatives of the third term in eqn (1).

For the description of the QM subsystem (and hence the excitation process itself) we use the coupled cluster (CC) approach. More specifically, we employ the approximate singles and doubles model CC2,[43] defined by (in a vacuum)

$$\begin{aligned} L_{\mathrm{CC2}} &= \left\langle \mathrm{HF}|\hat{H}\mathrm{e}^{-\hat{T}_1-\hat{T}_2}|\mathrm{HF}\right\rangle \\ &+ \sum_{\mu_1}\bar{t}_{\mu_1}\left\langle \mu_1|\mathrm{e}^{\hat{T}_1+\hat{T}_2}\hat{H}\mathrm{e}^{-\hat{T}_1-\hat{T}_2}|\mathrm{HF}\right\rangle \\ &+ \sum_{\mu_2}\bar{t}_{\mu_2}\left\langle \mu_2|[\hat{F},\hat{T}_2]+\mathrm{e}^{\hat{T}_1}\hat{H}\mathrm{e}^{-\hat{T}_1}|\mathrm{HF}\right\rangle, \end{aligned} \tag{2}$$

where $\hat{T}_1$ and $\hat{T}_2$ describe, respectively, single and double excitations out of the Hartree–Fock wavefunction (HF), $\hat{F}$ is the Fock operator, and $\bar{t}_{\mu_1}$ and $\bar{t}_{\mu_2}$ are Lagrangian multipliers. The factors on the Lagrangian multipliers are the standard CC2 equations. Recently, CC2 in its efficient resolution-of-the-identity (RI-CC2) variant[44] was combined with the PE approach to provide the PERI-CC2[37] method. A key factor in this development was to include both the second and the third term of eqn (1) such that (i) polarization effects are accounted for in both ground and excited states; (ii) the high computational efficiency of the RI-CC2 scheme for the QM part is preserved. This is achieved by replacing $\langle\hat{H}^{\mathrm{QM}}\rangle$ in eqn (1) with the CC2 Lagrangian of eqn (2) and introducing a special density defined for this purpose in the third term. The use of this special density is a slight modification of the general PE-CC theory, but is suitable in the context of RI-CC2 to preserve its efficiency and can be motivated by low-order correlation analysis similar in spirit to that of the vacuum CC2 model itself.[37]

In doing so, PERI-CC2 provides a particularly accurate and cost-efficient procedure for calculating excitation energies of complex systems. The use of PERI-CC2 in this work illustrates the potential of modern black-box approaches for describing excitation processes in biological systems.

In this work we calculate two-photon absorption transition strengths and not the two-photon absorption cross sections directly. However, since we only report relative quantities calculated at comparable wavelengths, the observations and conclusions regarding the transition strength will also apply to the cross section. The two-photon absorption transition strength is studied using the PE-DFT approach,[38] where $\langle\hat{H}^{\mathrm{QM}}\rangle$ and $\langle\hat{G}^{\mathrm{es}}\rangle$ as well as the term describing the polarization effects are evaluated using the density functional theory. In the absence of a two-photon absorption PERI-CC2 implementation the PE-DFT response approach is the best first-principles option, again using response theory for calculating excitation energies and properties (also commonly denoted TD-DFT). We use it in its CAM-B3LYP variant.[45] Besides improving issues related to charge-transfer excitations, CAM-B3LYP was found to give very accurate two-photon cross sections in benchmark calculations.[46] Even for extended chromophores, they are usually close to RI-CC2 results.[47] To the best of our knowledge this is the first time that two-photon properties are systematically investigated for retinal in a protein environment.

The actual calculations of the excitation energies are done using either PERI-CC2 as implemented very recently in the development version of the TURBOMOLE[48] package or by PE-DFT in the DALTON program.[49]

3 Computational details and preliminary studies

3.1 Preliminary RI-CC2 and DFT study of the retinal chromophore in isolation

In Table 1 we report RI-CC2 and DFT vertical excitation energies, E(exc), and relative two-photon absorption transition strengths, δ_{rel}, for the retinal chromophore model in isolation, *i.e.* no Lys chain is included and instead the retinylidene Schiff base is capped with a methyl group. This vacuum structure was obtained by performing a geometry optimization at B3LYP/cc-pVDZ level of theory using Gaussian 09.[50] For these studies we employed polarized double- and triple-ζ basis sets with diffuse functions developed by Pople and coworkers[51,52] and the correlation-consistent double-ζ basis sets[53] cc-pVDZ and aug-cc-pVDZ. For the RI-CC2 calculations we used the latter in combination with optimized auxiliary basis sets.[54] Based on Table 1 it seems reasonable to assume that basis set effects are small beyond 6-31+G* for the studied one-photon excitations described by DFT. Reasonable RI-CC2 results seem to be obtained using the cc-pVDZ basis set and have been used for the remaining PERI-CC2 calculations in this study. Accurate results for the two-photon transition strength (described by DFT) required the use of the slightly larger 6-311+G* basis. For further benchmarks of RI-CC2 for similar biological chromophores, see Send *et al.*[35]

It has been found in experiments that retinal absorbs at 2.0 eV.[55] In comparison, TD-DFT(CAM-B3LYP) predicts an excitation energy of ≈2.4 eV while RI-CC2/aug-cc-pVDZ gives an excitation energy slightly above 2.1 eV. These values are in good agreement with previous studies of retinal in the gas phase based on CC2.[34,35] This accuracy is about what can be expected in view of the inherent errors of these methods and

Table 1 Basis set investigation for the retinal chromophore model in a vacuum using DFT(CAM-B3LYP) and RI-CC2. Given are the number of basis functions (# b.f.), the excitation energy (E(exc)) and the relative two-photon transition strength (δ_{rel})

Basis set	# b.f.	E(exc)/eV	δ_{rel} [a]
DFT			
6-31+G*	460	2.43	1.03
6-311+G*	580	2.43	1.00
6-311++G**	708	2.42	1.00
aug-cc-pVDZ	794	2.42	1.00
RI-CC2			
SVP	468	2.16	—
cc-pVDZ	468	2.17	—
aug-cc-pVDZ	794	2.13	—

[a] $\delta_{\mathrm{rel}} = \delta_{\mathrm{basis}}/\delta_{\text{6-311+G*}}$.

Published on 27 March 2013. Downloaded by Ruhr Universitat Bochum on 1/16/2019 10:21:45 AM.

the comparison of vertical excitation energies with experimental band maxima. The trends of the errors are consistent with the experience in the literature: a small blue shift (0.1 eV) of the CC2 and a slightly larger blue shift (0.4 eV) of the CAM-B3LYP results.

3.2 Molecular structures

It is the recent publication[14] of a highly resolved geometry that allows us to make the following predictions of spectral trends of amino acids within the ChR binding pocket. Indeed, in an atomic description of the surrounding as in the PE model, it is essential that the underlying 3D structure is reliable in order to draw conclusions on its predictive power.

Before it can be used for quantum chemical calculations the experimental structure needs to be refined. We started from the C1C2 structure as obtained from the PDB database[56] with access number 3UG9.[14] The protein structure was prepared using the protein preparation wizard in the Schrödinger software graphical interface Maestro.[57–61] Hydrogen atoms, missing side chains and loops were added during the preprocessing phase. The positions of the hydrogen atoms were optimized using the OPLS2005 force field.[62,63] Subsequently, the hydrogen bond assignment using exhaustive sampling, including water orientation, and optimization of hydrogen bond lengths and angles of the altered species were performed. The result of the protein preparation was that all residues have standard protonation states except for E129 which was neutral and H139 and H173 which were positive. The imidazole rings of the H139, H311, H313 and H317 residues were flipped, together with the side chain amides of N69, N92, Q112, N185, Q249 and N327 residues. The protonation state of H311 was adjusted to the epsilon nitrogen position. Finally, an additional optimization of the hydrogen atom positions was performed using MacroModel[64] with the OPLS2005 force field, water solvation, and a tighter convergence threshold on the root-mean-square (RMS) gradient of the energy (0.001 kJ mol^{-1} $Å^{-1}$). The PDB crystal structure includes two flipped states of F133 (A and B). We performed PE calculations on both the A and B forms (not shown) and concluded that the flipping effect was minor (<0.005 eV) on the relevant excitation energy. Therefore, we only make use of the A form in the final calculations.

After the initial preparation we refined the retinal structure using QM/MM optimization at the B3LYP/6-31+G* level of theory combined with the OPLS2005 force field. During the QM/MM optimization the protein environment was kept fixed to ensure that the final structure was close to the experimentally determined structure while still producing accurate geometries of the retinal chromophore. For these QM/MM geometry optimizations we have used the QSite program.[65–67] The size of the QM region was justified by performing a series of test calculations as detailed in the following section.

3.3 Size of the QM region

The size of the QM region is always a critical choice in PE calculations (and QM/MM in general). We have investigated five different model systems for the QM region. Note that the first four model systems are positively charged while the final (largest) is negatively charged due to the explicit inclusion of the Glu162 and Asp292 counter ions into the QM region. There are two different domains where the size of the QM region needs to be determined: (1) the QM/MM geometry optimization (if any) and (2) the subsequent PE-QM calculation. In Table 2 these two QM regions are referred to as QMopt and QMpe, respectively. In model 1 we perform the PE-QM calculation directly on the crystal structure, prepared as described in the previous section, using the retinylidene Schiff base capped with a methyl group as the QM system. In the different models we subsequently incorporate the covalently bonded Lys residue as well as the chemically more important amino acids into the QM regions (both in the QM/MM optimization and the PE-QM calculations). We observe that model 4 has a good compromise between accuracy and cost and we thus proceed with this QM region in all remaining calculations. An important geometrical feature is the bond length alternation (BLA), *i.e.* the difference between the mean single and double bond length in a conjugated alkene chain. See the ESI† for a detailed definition of BLA for *all-trans* retinal. Note the decrease of BLA upon the QM/MM geometry optimization suggesting that the planarity of retinal is somewhat perturbed in the crystal structure generation.

3.4 The embedding potentials

In the PE calculations of the one- and two-photon absorption properties, the effects from the protein surrounding are modelled by embedding potentials that consist of localized atom-centred multipole moments up to quadrupoles and anisotropic dipole–dipole polarizabilities. The derivation of the parameters involves three steps: first, the protein is fragmented into single amino acid residues and the broken bonds are saturated with acetyl and *N*-methyl capping groups.[68,69] Second, the calculation of the localized atom-centred parameters of the different

Table 2 Investigation on the size dependence of the chosen QM region. We use five different setups to investigate bond length alternation (BLA), excitation energy (E(exc)) and relative two-photon transition strengths (δ_{rel}). See the text for further details

Model	QMopt	QMpe	BLA/Å	E(exc)/eV	δ_{rel} [a]
1	—	Ret + $NHCH_3$	0.13	2.70	1.0
2	Ret + $NHCH_3$	Ret + $NHCH_3$	0.07	2.82	0.5
3	Ret + K296 + D292 + E162 + HOH + W163	Ret + $NHCH_3$	0.08	2.85	0.6
4	Ret + K296 + D292 + E162 + HOH + W163	Ret + K296	0.08	2.91	0.4
5	Ret + K296 + D292 + E162 + HOH + W163	Ret + K296 + D292 + E162 + HOH + W163	0.08	2.89	0.5

[a] $\delta_{rel} = \delta_{model\ i}/\delta_{model\ 1}$.

 This journal is © the Owner Societies 2013

Published on 27 March 2013. Downloaded by Ruhr Universitat Bochum on 1/16/2019 10:21:45 AM.

Table 3 Investigation of the effect of different embedding potentials for determining the relevant excitation energy (E(exc)) in C1C2 ChR based on various levels of theory

Model		E(exc)/eV
m0p0	B3LYP/6-31+G*	3.09
m2p0	B3LYP/6-31+G*	3.07
m2p1	B3LYP/6-31+G*	2.93
m2p2	B3LYP/6-31+G*	2.91
resp-p0	HF/6-31G*	3.09
resp-p1	B3LYP/cc-pVTZ	2.95

fragments is done using the LoProp[70] approach implemented in Molcas.[71] These calculations were performed at B3LYP/6-31+G* level of theory using a atomic natural orbital (ANO) type recontraction of the 6-31+G* basis set which is required by the LoProp method.[70] Finally, in the third step the final parameters are derived by recombining the protein and properly subtracting capping group effects. The accuracy of the LoProp potentials for a series of solvent molecules and amino acids has been thoroughly studied before and it was found that the quantum mechanical electrostatic potential can be accurately reproduced at the interaction distances of interest.[38,72,73] Furthermore, the quality of protein potentials derived using the fragmentation procedure as described above has been validated recently.[74]

We have investigated the effect of different force field descriptions on the excitation energy. The results are compiled in Table 3 where we use a notation specifying the order of the distributed multipoles (m = 0 for charges, m = 1 for charges + dipoles, *etc.*) and the type of polarizability (p = 0 for none, p = 1 for isotropic, p = 2 for anisotropic). The LoProp force fields were generated using the approach defined in ref. 69. We compared them with force fields where the multipoles were replaced with electrostatic potential fitted point charges derived using the restrained electrostatic potential (RESP) fitting procedure.[75,76] Both types of force fields emphasize the importance of including explicit polarization effects in the environment description. The LoProp m2p2 potential was used in the remaining PE excitation energy calculations.

3.5 The mutation protocol

We shall in this work use a non-standard approach to rational protein design by performing site-specific mutations on a computer.

From the non-mutated structure we create a series of different structures where one or two residues are mutated. Each of these mutated structures perturbs the excited state properties of retinal in a slightly different manner. For each of these unique inputs we may then perform PE calculations detailing the effects of the different amino acids for tuning the absorption properties. Note that one could alternatively choose only to include one amino acid at a time (instead of all of them) in the surroundings description. However, such an approach will not incorporate the mutual (many-body) interaction between the amino acids themselves and we thus refrain from it here. Previously, similar mutation-type studies – referred to as a perturbation analysis – have been carried out for other rhodopsin proteins.[28,77] Further, somewhat related to this study are two very recent investigations[15,16] of the credibility of (non-polarizable) QM/MM methods for predicting colour change in a rhodopsin training system.

To model a mutant, we start from the QM/MM optimized structure which has been obtained as described in the previous sections. Then, the amino acid(s) corresponding to the point mutation(s) of choice is replaced accordingly in the MM region. For all variants involving mutations to a glycine residue, which corresponds to the removal of the side chain, the bond length between the alpha carbon and the hydrogen atom replacing the side chain was scaled to 1.09 Å while keeping the direction of the bond intact. For all other mutations we performed a force field geometry optimization keeping everything fixed except the mutated residue. The optimizations were performed using MacroModel[64] with the OPLS2005 force field and an increased convergence threshold of 0.001 kJ mol^{-1} $Å^{-1}$ on the RMS gradient of the energy. To complete the m2p2 potential, the necessary computations are carried out for the new amino acid(s) and the new parameters are fit into the remaining protein potential which has already been obtained for the non-mutated structure.

4 Results and discussion

4.1 Effects that influence the excitation energy and two-photon transition strength in ChR

The unique properties of retinal are closely associated with its ability to absorb light at different wavelengths depending on its molecular surrounding. An important first step towards understanding the absorption properties is the dissection of the contributions into steric effects (*i.e.* the change in geometry for retinal inside the protein compared to the isolated planar structure of *all-trans* retinal) and the more direct electrostatic effects stemming from the interaction with the charge distribution of the amino acids in the protein. To answer this consider the change in geometry depicted in Fig. 1 obtained by superimposing the relaxed structure in isolation and the structure

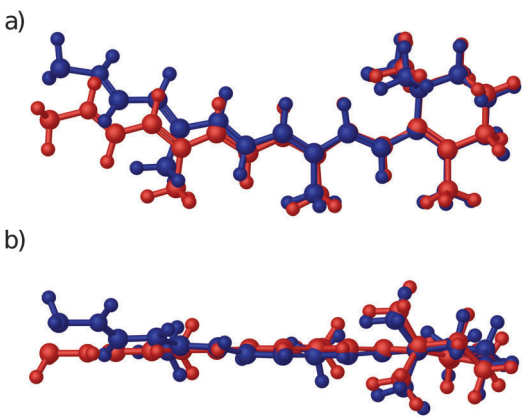


Fig. 1 Change in planarity going from the vacuum structure (red) to that found within the protein (blue).

Published on 27 March 2013. Downloaded by Ruhr Universitat Bochum on 1/16/2019 10:21:45 AM.

Table 4 Overview of the factors influencing the channel-opening excitation energy of C1C2 as well as the relative two-photon transition strength (linearly polarized light)

Environment		PERI-CC2	PE-DFT	
Effect	Description	E(exc)/eV	E(exc)/eV	δ_{rel} [a]
Vacuum	vac.	2.16	2.42	1.0
Steric	vac.	2.11	2.43	3.1
Electrostatics	m2p0	3.21	3.07	0.6
Polarization	m2p2	3.00	2.91	1.0

[a] $\delta_{rel} = \delta/\delta_{vac}$.

observed inside the protein. Going from the vacuum to the in-protein geometry the BLA increases approximately 0.05 Å indicating only a small decrease in the amount of conjugation – see also Table 2. A similar increase in BLA is also observed for related rhodopsin proteins.[27,28] For the vertical excitation energy, the steric effects convey a small change (relative to the isolated retinal) of approximately −0.05 eV (see Table 4). In contrast, the charge distribution in the surrounding, *i.e.* incorporating the amino acids, markedly influences the excitation energy blue-shifting it by 0.84 eV compared to the vacuum. This leads to the conclusion that – similar to related rhodopsin studies[15,16,19–30] – the environment provides the primary handle for colour tuning. As an aside, note that polarization effects have nonzero contributions to the shift, lowering the excitation energy by 0.21 eV with respect to the non-polarizable embedding (m2p0). This is in agreement with earlier studies[78,79] demonstrating that quantitative agreement for shifts requires the inclusion of polarization effects. It is noteworthy that the geometry effects have a much larger influence on the two-photon transition strength, δ, where our calculations – see Table 4 – predict that the large two-photon cross section inside the protein results from a balance between geometry effects (serving to increase the cross section) and that of the environment.

4.2 Describing the absorption properties of known ChR mutants

The hunt for optically tuned ChR is already well under way resulting in a toolbox of ChR variants each absorbing at somewhat different wavelengths.[8–13] In order to demonstrate the reliability of the mutation protocol for yielding predictive absorption results, we report in Table 5 the results of PERI-CC2 calculations. First of all, we observe how the qualitative trends reported in experiment[8,10] are well reproduced by the computational approach. Vertical excitation energies are compared to experimental excitation energies at maximum absorption. For instance, we observe the favourable red-shift of the T198C/E162T (ChETA) mutant which has earned it a high-ranking place among the available ChR2 variants.[7] We also predict that this particular mutant possesses an even larger two-photon cross section than observed in ChR thus making it an ideal candidate for further studies of two-photon activated optogenetics. Generally, it seems that PERI-CC2 consistently overestimates the spectral shift. However, we emphasize that the simple perturbational approach to mutation studies taken here performs remarkably well in reproducing the experimental reference data.

Table 5 Mutations serving to validate the computational approach. All calculated excitation energy shifts (ΔE(exc)) are based on PERI-CC2; relative changes in two-photon transition strengths ($\Delta\delta$) are computed using PE-DFT. The experimental references are taken from the literature as indicated

	ΔE(exc)[a]/eV		
Mutation	Calc.	Exp.	$\Delta\delta_{rel}$ [b] (%)
T198C	−0.02	∼0.00[c]	+20
T198C/E162T	−0.32	∼−0.18[c]	+150
H173R	0.04	∼0.00[c]	+0
E162A	−0.30	∼−0.11[d]	+120
E162D	−0.07	∼−0.05[d]	+30
E162Q	−0.42	∼−0.16[d]	+160
E162T	−0.27	∼−0.16[d]	+120

[a] $\Delta E(\text{exc}) = E(\text{exc})_{mutant} - E(\text{exc})_{C1C2}$. [b] $\Delta\delta_{rel} = (\delta_{mutant} - \delta^{C1C2})/\delta^{C1C2}$. [c] Ref. 8. [d] Ref. 10.

4.3 Perturbational effects of amino acids in the binding pocket

The next step along the way of designing optically tuned ChR variants is the mapping of the dominating electrostatic effects of the amino acids in the protein; in particular those close to retinal. Specifically, to which amino acids can we assign the largest changes in the excitation energy? In Fig. 2 we illustrate the importance of several amino acids (or rather their side chains) for tuning purposes in terms of the shifts $E(\text{exc})_{mutant} - E(\text{exc})_{C1C2}$ for the mutants obtained by replacing a given amino acid with glycine. The mutants have been sorted by distance from the substituted amino acid to the Schiff base N. As expected, the close lying charged residues (Asp292 and Glu162) – also constituting the counter ion complex – have the largest tuning effect of approximately −0.3 eV each. Note that a negative spectral shift suggests that the mutant with glycine absorbs at

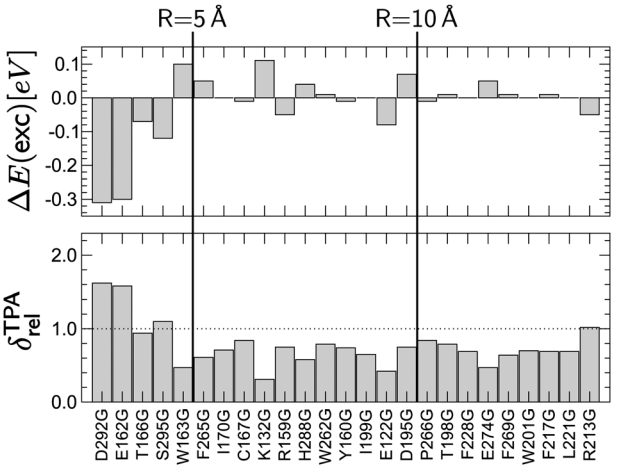


Fig. 2 The spectral shift and two-photon transition strength change of the Gly mutants relative to C1C2 sorted by distance to Schiff base N (closest first). All excitation energies are calculated using PERI-CC2 while the transition strength is calculated using PE-DFT.

 This journal is © the Owner Societies 2013

Published on 27 March 2013. Downloaded by Ruhr Universitat Bochum on 1/16/2019 10:21:45 AM.

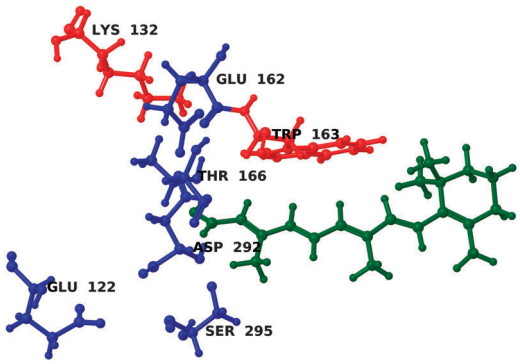


Fig. 3 Illustration of retinal (green) surrounded by the amino acids that affect the spectral shift by at least 0.07 eV. Residues that have an overall red-shifting effect (relative to glycine) are coloured red and those that have a blue-shifting effect are coloured blue.

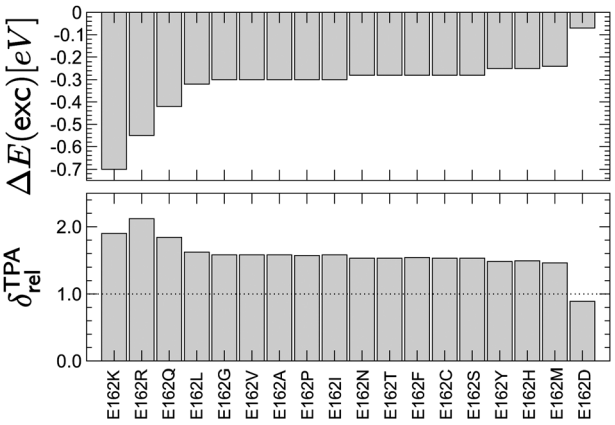


Fig. 4 The spectral shift and change in two-photon transition strength of the E162X mutants. Ordered by the size of the spectral shift.

longer wavelengths than C1C2. This indicates that *e.g.* Asp292 has a blue-shifting effect (since D292G is red-shifted) on the excitation energy. That being said, it is striking that all residues give rise to relatively small shifts (in either direction). We have also investigated the effects of three close-lying (to retinal) water molecules by removing them from the calculation. In all three cases we observe changes in the excitation energy smaller than 0.05 eV. More insight is obtained in Fig. 3 where we have depicted the residues in the binding pocket contributing at least 0.07 eV (10 nm) to the tuning of the excitation energy. The residues found to give a significant spectral shift are located at the Schiff base N-end of retinal. Accumulation of charged residues in the Schiff base N region leads to a smaller absorption wavelength, while replacement of charged residues with neutral ones (D292G, say) red-shifts the excitation energy.

In Fig. 2 we also report the enhancement ratios $\delta^{\mathrm{mutant}}/\delta^{\mathrm{C1C2}}$ for the two-photon transition strength relative to C1C2 using the same set of artificially created mutants. Again, amino acids constituting the complex counter ion have the largest effect, by far. Indeed, it seems that the Asp292 and Glu162 residues are the primary reason that the transition strength is decreased so much compared to the retinal structure without a surrounding embedding potential – see Table 4. Along this line, the results indicate that the remaining amino acids play the same quenching role as observed for the tuning of the excitation energy.

4.4 Tuning the absorption properties

From Fig. 2 and 3 it is clear that the close-lying counter-ions have the largest tuning potential for the excitation energy. In fact, it seems that the only viable options to obtain measurable red-shifts are Asp292 and Glu162. However, Asp292 is speculated to be the primary proton acceptor in ChR2[14] most likely leading to functional loss upon mutation. Glu162, on the other hand, may be manipulated at will without a significant decrease in the characteristic photo-current.[10] Indeed, this has also been found using a straightforward trial-and-error approach to mutation and ultimately leads to the experimentally expressed ChR2 variants listed in Table 5. Consequently, one approach that suggests itself is to investigate the tuning potential of Glu162 by scanning the full set of all possible amino acids. While tedious and time-consuming to perform in the lab, such an exercise readily lends itself to being investigated on a computer. In Fig. 4 we systematically investigate the changes in the excitation energy as well as in the two-photon transition strength. First, for most of the mutants the shift is approximately identical, in agreement with the fact that the different residues act very similar to perturbations. Second, observe that the conservatory mutation E162D yields similar absorption properties as the wild type as expected given the similarity between glutamic and aspartic acid. Evidently, the only mutations that introduce the wanted red-shift are E162K and E162R. Lysine and arginine share the features of being positively charged and relatively large. Indeed, taken together these factors suggest that both mutations most likely are unrealistic, essentially because the substitutions may no longer be seen as simple perturbations which was the assumption from the outset. To some extent substitution to glutamine (basically amounting to changing an OH to an NH_2 group) also results in a favourable red-shift as also seen experimentally.[10]

The conclusion from these observations is clear: it is doubtful that few-site mutations can lead to shifts large enough to make ChR2 applicable to *in vivo* applications that require shifts of around 0.45 eV. Instead, techniques such as helix swapping probably need to be followed. VChR1 is an excellent example of this, demonstrating a red-shifted excitation energy of approximately 0.35 eV.[9] Along this line it is also interesting to comment on the potential of obtaining combinatory spectral control in the same physical volume, *i.e.* is it possible to design two ChR variants that have negligible overlap of their spectral profiles allowing for completely novel optogenetic experiments? To this end, one strategy[9] is to rely on the VChR1 chimera as well as a blue-shifted variant of ChR2. Fig. 2 also gives insight into the design of the latter since we observe that the amino acids primarily responsible for the red-shift are Trp163 and Lys132. However, in both cases their tuning effect is rather limited and forces us to conclude the same as for

Published on 27 March 2013. Downloaded by Ruhr Universitat Bochum on 1/16/2019 10:21:45 AM.

designing red-shifted mutants: single-site mutations are probably not a feasible strategy if a significant blue-shift is needed.

5 Conclusions

The photo-activated channelrhodopsin (ChR) membrane protein is the cornerstone of the increasingly popular field of optogenetics. Recently, Kato *et al.*[14] reported an X-ray structure of the ChR binding pocket. In this contribution we have performed a high-level *in silico* mutagenesis screening study – based on the aforementioned C1C2 crystal structure – using polarizable embedding QM/MM theory in combination with coupled cluster and density functional theory as QM methods. In particular, this work is the first application of the recently developed PERI-CC2 method.

The results provide us with a catalogue of the spectral effects of individual amino acids in the protein. In turn we are able to address two important points: (i) the potential for tuning the excitation energy to different wavelengths (preferably higher) and (ii) the potential for enhancing the two-photon absorption cross section of retinal inside ChR. While point (i) may immediately stimulate further research in the continued attempt of molecular engineering of ChR variants, point (ii) touches on an area that has only received scarce attention experimentally and none at all computationally. Overall, one of our main conclusions corroborates what has also been found using a more trial-and-error approach to mutation studies:[5] it is fundamentally difficult – based on only single or double mutations – to shift the photospectrum by more than 0.05–0.15 eV. Indeed, based on the studied mutations we conjecture that it will prove near to impossible to meet the experimental demand[3] of significantly red-shifted absorption spectra using single-site mutation strategies. With regards to the use of two-photon techniques for activating ChR we advocate the use of the ChETA double mutant conjectured here to have an even larger two-photon cross section than the ChR2 wildtype version.

Finally, this work illustrates how PERI-CC2 can be used for quickly scanning possible candidates before further experimental mutation studies are conducted. Indeed, with the complementary information obtained from computations one may limit the number of mutants that are actually synthesized and characterized and thereby save a great deal of both time and money in the long run.

Acknowledgements

O.C. acknowledges support from the Danish Center for Scientific Computing (DCSC), the Danish national research foundation, the Lundbeck Foundation and EUROHORCs for a EURYI award. J.K. thanks the Danish Center for Scientific Computing (DCSC), The Danish Councils for Independent Research (STENO and Sapere Aude programmes), the Lundbeck Foundation and the Villum foundation for financial support. C.H. acknowledges financial support from Deutsche Forschungsgemeinschaft through grant HA 2588/6 and the Cluster of Excellence RESOLV (EXC 1069).

References

1 E. S. Boyden, F. Zhang, E. Bamberg, G. Nagel and K. Deisseroth, *Nat. Neurosci.*, 2005, **8**, 1263–1268.
2 X. Li, D. V. Gutierrez, M. G. Hanson, J. Han, M. D. Mark, H. Chiel, P. Hegemann, L. T. Landmesser and S. Herlitze, *Proc. Natl. Acad. Sci. U. S. A.*, 2005, **102**, 17816–17821.
3 K. Deisseroth, *Nat. Methods*, 2011, **8**, 26–29.
4 *Nat. Methods*, 2011, **8**, 1.
5 F. Zhang, J. Vierock, O. Yizhar, L. E. Fenno, S. Tsunoda, A. Kianianmomeni, M. Prigge, A. Berndt, J. Cushman, J. Polle, J. Magnuson, P. Hegemann and K. Deisseroth, *Cell*, 2011, **147**, 1446–1457.
6 P. Hegemann and A. Möglich, *Nat. Methods*, 2011, **8**, 39–42.
7 L. Fenno, O. Yizhar and K. Deisseroth, *Annu. Rev. Neurosci.*, 2011, **34**, 389–412.
8 A. Berndt, P. Schoenenberger, J. Mattis, K. M. Tye, K. Deisseroth, P. Hegemann and T. G. Oertner, *Proc. Natl. Acad. Sci. U. S. A.*, 2011, **108**, 7595–7600.
9 F. Zhang, M. Prigge, F. Beyrière, S. P. Tsunoda, J. Mattis, O. Yizhar, P. Hegemann and K. Deisseroth, *Nat. Neurosci.*, 2008, **11**, 631–633.
10 L. A. Gunaydin, O. Yizhar, A. Berndt, V. S. Sohal, K. Deisseroth and P. Hegemann, *Nat. Neurosci.*, 2010, **13**, 387–392.
11 S. P. Tsunoda and P. Hegemann, *Photochem. Photobiol.*, 2009, **85**, 564–569.
12 J. Y. Lin, M. Z. Lin, P. Steinbach and R. Y. Tsien, *Biophys. J.*, 2009, **96**, 1803–1814.
13 A. Berndt, O. Yizhar, L. A. Gunaydin, P. Hegemann and K. Deisseroth, *Nat. Neurosci.*, 2009, **12**, 229–234.
14 H. E. Kato, F. Zhang, O. Yizhar, C. Ramakrishnan, T. Nishizawa, K. Hirata, J. Ito, Y. Aita, T. Tsukazaki, S. Hayashi, P. Hegemann, A. D. Maturana, R. Ishitani, K. Deisseroth and O. Nureki, *Nature*, 2012, **482**, 369–374.
15 F. Melaccio, N. Ferré and M. Olivucci, *Phys. Chem. Chem. Phys.*, 2012, **14**, 12485–12495.
16 M. Kamiya, H. E. Kato, R. Ishitani, O. Nureki and S. Hayashi, *Chem. Phys. Lett.*, 2013, **556**, 266–271.
17 J. P. Rickgauer and D. W. Tank, *Proc. Natl. Acad. Sci. U. S. A.*, 2009, **106**, 15025–15030.
18 E. Papagiakoumou, F. Anselmi, A. Bègue, V. Sars, J. Glückstad, E. Y. Isacoff and V. Emiliani, *Nat. Methods*, 2010, **7**, 848–854.
19 M. N. Ryazantsev, A. Altun and K. Morokuma, *J. Am. Chem. Soc.*, 2012, **134**, 5520–5523.
20 P. B. Coto, A. Strambi, N. Ferré and M. Olivucci, *Proc. Natl. Acad. Sci. U. S. A.*, 2006, **103**, 17154–17159.
21 K. Fujimoto, S. Hayashi, J. Hasegawa and H. Nakatsuji, *J. Chem. Theory Comput.*, 2007, **3**, 605–618.
22 M. Schreiber, V. Bußand M. Sugihara, *J. Chem. Phys.*, 2003, **119**, 12045–12048.
23 M. Wanko, M. Hoffmann, P. Strodel, A. Koslowski, W. Thiel, F. Neese, T. Frauenheim and M. Elstner, *J. Phys. Chem. B*, 2005, **109**, 3606–3615.

 This journal is © the Owner Societies 2013

Published on 27 March 2013. Downloaded by Ruhr Universitat Bochum on 1/16/2019 10:21:45 AM.

24 L. Lasogga, W. Rettig, H. Otto, I. Wallat and J. Bricks, *J. Phys. Chem. A*, 2010, **114**, 2179–2188.
25 V. R. I. Kaila, R. Send and D. Sundholm, *J. Phys. Chem. B*, 2012, **116**, 2249–2258.
26 G. Tomasello, G. Olaso-González, P. Altoè, M. Stenta, L. Serrano-Andrés, M. Merchán, G. Orlandi, A. Bottoni and M. Garavelli, *J. Am. Chem. Soc.*, 2009, **131**, 5172–5186.
27 A. Altun, S. Yokoyama and K. Morokuma, *J. Phys. Chem. B*, 2008, **112**, 6814–6827.
28 M. Hoffmann, M. Wanko, P. Strodel, P. H. König, T. Frauenheim, K. Schulten, W. Thiel, E. Tajkhorshid and M. Elstner, *J. Am. Chem. Soc.*, 2006, **128**, 10808–10818.
29 K. Bravaya, A. Bochenkova, A. Granovsky and A. Nemukhin, *J. Am. Chem. Soc.*, 2007, **129**, 13035–13042.
30 A. Altun, S. Yokoyama and K. Morokuma, *J. Phys. Chem. B*, 2008, **112**, 16883–16890.
31 A. J. A. Aquino, M. Barbatti and H. Lischka, *ChemPhysChem*, 2006, **7**, 2089–2096.
32 R. Send and D. Sundholm, *J. Phys. Chem. A*, 2007, **111**, 27–33.
33 R. Send and D. Sundholm, *J. Phys. Chem. A*, 2007, **111**, 8766–8773.
34 Y. Kawashima, H. Nakano, J. Jung and S. Ten-no, *Phys. Chem. Chem. Phys.*, 2011, **13**, 11731–11738.
35 R. Send, V. R. I. Kaila and D. Sundholm, *J. Chem. Theory Comput.*, 2011, **7**, 2473–2484.
36 R. Send, V. R. I. Kaila and D. Sundholm, *J. Chem. Phys.*, 2011, **134**, 214114.
37 T. Schwabe, K. Sneskov, J. M. H. Olsen, J. Kongsted, O. Christiansen and C. Hättig, *J. Chem. Theory Comput.*, 2012, **8**, 3274–3283.
38 J. M. Olsen, K. Aidas and J. Kongsted, *J. Chem. Theory Comput.*, 2010, **6**, 3721–3734.
39 A. Warshel and M. Levitt, *J. Mol. Biol.*, 1976, **103**, 227–249.
40 J. M. H. Olsen and J. Kongsted, *Adv. Quantum Chem.*, 2011, **61**, 107–143.
41 K. Sneskov, T. Schwabe, J. Kongsted and O. Christiansen, *J. Chem. Phys.*, 2011, **134**, 104108.
42 K. Sneskov, T. Schwabe, O. Christiansen and J. Kongsted, *Phys. Chem. Chem. Phys.*, 2011, **13**, 18551–18560.
43 O. Christiansen, H. Koch and P. Jørgensen, *Chem. Phys. Lett.*, 1995, **243**, 409.
44 C. Hättig and F. Weigend, *J. Chem. Phys.*, 2000, **113**, 5154–5161.
45 T. Yanai, D. P. Tew and N. C. Handy, *Chem. Phys. Lett.*, 2004, **393**, 51–57.
46 M. J. Paterson, O. Christiansen, F. Pawlowski, P. Jørgensen, C. Hättig, T. Helgaker and P. Sałek, *J. Chem. Phys.*, 2006, **124**, 054322.
47 D. H. Friese, C. Hättig and K. Ruud, *Phys. Chem. Chem. Phys.*, 2012, **14**, 1175–1184.
48 TURBOMOLE V6.4 2012, a development of University of Karlsruhe and Forschungszentrum Karlsruhe GmbH, 1989–2007, TURBOMOLE GmbH, since 2007; available at http://www.turbomole.com.
49 DALTON, a molecular electronic structure program, Release Dalton2011 (2011), see http://daltonprogram.org/.
50 M. J. Frisch, G. W. Trucks, H. B. Schlegel, G. E. Scuseria, M. A. Robb, J. R. Cheeseman, G. Scalmani, V. Barone, B. Mennucci, G. A. Petersson, H. Nakatsuji, M. Caricato, X. Li, H. P. Hratchian, A. F. Izmaylov, J. Bloino, G. Zheng, J. L. Sonnenberg, M. Hada, M. Ehara, K. Toyota, R. Fukuda, J. Hasegawa, M. Ishida, T. Nakajima, Y. Honda, O. Kitao, H. Nakai, T. Vreven, J. A. Montgomery, Jr., J. E. Peralta, F. Ogliaro, M. Bearpark, J. J. Heyd, E. Brothers, K. N. Kudin, V. N. Staroverov, R. Kobayashi, J. Normand, K. Raghavachari, A. Rendell, J. C. Burant, S. S. Iyengar, J. Tomasi, M. Cossi, N. Rega, J. M. Millam, M. Klene, J. E. Knox, J. B. Cross, V. Bakken, C. Adamo, J. Jaramillo, R. Gomperts, R. E. Stratmann, O. Yazyev, A. J. Austin, R. Cammi, C. Pomelli, J. W. Ochterski, R. L. Martin, K. Morokuma, V. G. Zakrzewski, G. A. Voth, P. Salvador, J. J. Dannenberg, S. Dapprich, A. D. Daniels, Ö. Farkas, J. B. Foresman, J. V. Ortiz, J. Cioslowski and D. J. Fox, *Gaussian 09 Revision A.1*, Gaussian Inc., Wallingford, CT, 2009.
51 W. J. Hehre, R. Ditchfield and J. A. Pople, *J. Chem. Phys.*, 1972, **56**, 2257.
52 R. Krishnan, J. S. Blinkley, R. Seeger and J. A. Pople, *J. Chem. Phys.*, 1980, **72**, 650.
53 T. H. Dunning, *J. Chem. Phys.*, 1989, **90**, 1007.
54 F. Weigend, A. Köhn and C. Hättig, *J. Chem. Phys.*, 2002, **116**, 3175–3183.
55 I. B. Nielsen, L. Lammich and L. H. Andersen, *Phys. Rev. Lett.*, 2006, **96**, 018304.
56 H. M. Berman, J. Westbrook, Z. Feng, G. Gilliland, T. N. Bhat, H. Weissig, I. N. Shindyalov and P. E. Bourne, *Nucleic Acids Res.*, 2000, **28**, 235–242.
57 Schrödinger Suite 2011 Protein Preparation Wizard, Schrödinger, LLC, New York, NY, 2011.
58 *Epik, version 2.2*, Schrödinger, LLC, New York, NY, 2011.
59 *Impact, version 5.7*, Schrödinger, LLC, New York, NY, 2011.
60 *Prime, version 3.0*, Schrödinger, LLC, New York, NY, 2011.
61 *Maestro, version 9.2*, Schrödinger, LLC, New York, NY, 2011.
62 J. L. Banks, H. S. Beard, Y. Cao, A. E. Cho, W. Damm, R. Farid, A. K. Felts, T. A. Halgren, D. T. Mainz, J. R. Maple, R. Murphy, D. M. Philipp, M. P. Repasky, L. Y. Zhang, B. J. Berne, R. A. Friesner, E. Gallicchio and R. M. Levy, *J. Comput. Chem.*, 2005, **26**, 1752.
63 G. A. Kaminski, R. A. Friesner, J. Tirado-Rives and W. L. Jorgensen, *J. Phys. Chem. B*, 2001, **105**, 6474–6487.
64 *MacroModel, version 9.9*, Schrödinger, LLC, New York, NY, 2011.
65 *QSite, version 5.7*, Schrödinger, LLC, New York, NY, 2011.
66 R. B. Murphy, D. M. Philipp and R. A. Friesner, *J. Comput. Chem.*, 2000, **21**, 1442–1457.
67 D. M. Philipp and R. A. Friesner, *J. Comput. Chem.*, 1999, **20**, 1468–1494.
68 D. W. Zhang and J. Z. H. Zhang, *J. Chem. Phys.*, 2003, **119**, 3599–3605.

Published on 27 March 2013. Downloaded by Ruhr Universitat Bochum on 1/16/2019 10:21:45 AM.

69 P. Söderhjelm and U. Ryde, *J. Phys. Chem. A*, 2009, **113**, 617–627.
70 L. Gagliardi, R. Lindh and G. Karlström, *J. Chem. Phys.*, 2004, **121**, 4494–4500.
71 F. Aquilante, L. De Vico, N. Ferré, G. Ghigo, P.-Å. Malmqvist, P. Neogrády, T. B. Pedersen, M. Pitoňák, M. Reiher, B. O. Roos, L. Serrano-Andrés, M. Urban, V. Veryazov and R. Lindh, *J. Comput. Chem.*, 2010, **31**, 224–247.
72 P. Söderhjelm, J. W. Krogh, G. Karlström, U. Ryde and R. Lindh, *J. Comput. Chem.*, 2007, **28**, 1083–1090.
73 T. Schwabe, J. M. Olsen, K. Sneskov, J. Kongsted and O. Christiansen, *J. Chem. Theory Comput.*, 2011, **7**, 2209–2217.
74 J. M. H. Olsen, *Development of Quantum Chemical Methods towards Rationalization and Optimal Design of Photoactive Proteins*, PhD Thesis, University of Southern Denmark, 2012, DOI: 10.6084/m9.figshare.156852.
75 C. I. Bayly, P. Cieplak, W. Cornell and P. A. Kollman, *J. Phys. Chem.*, 1993, **97**, 10269–10280.
76 J. Wang, W. Wang, P. A. Kollman and D. A. Case, *J. Mol. Graphics Modell.*, 2006, **25**, 247–260.
77 K. Welke, J. S. Frähmcke, H. C. Watanabe, P. Hegemann and M. Elstner, *J. Phys. Chem. B*, 2011, **115**, 15119–15128.
78 M. Wanko, M. Hoffmann, T. Frauenheim and M. Elstner, *J. Phys. Chem. B*, 2008, **112**, 11462–11467.
79 M. Sakurai, K. Sakata, S. Saito, S. Nakajima and Y. Inoue, *J. Am. Chem. Soc.*, 2003, **125**, 3108–3112.

 This journal is © the Owner Societies 2013